**Showcasing research from the labs of Professor Hiroki Oguri, Department of Applied Chemistry, Graduate School of Engineering, Tokyo University of Agriculture & Technology, Tokyo, Japan, and Professor Satoshi Maeda, Department of Chemistry, Faculty of Science & Institute for Chemical Reaction Design and Discovery (WPI-ICReDD), Hokkaido University, Sapporo, Japan.**

Zn(OTf)$_2$-mediated annulations of *N*-propargylated tetrahydrocarbolines: divergent synthesis of four distinct alkaloidal scaffolds

A programmable divergent synthesis of four distinct alkaloidal scaffolds was implemented by Zn(OTf)$_2$-mediated intramolecular annulations between indole C2/C3 positions and the internal/distal alkynyl carbons as well as an unexpected α-alkenylation of a carbonyl group. Use of the artificial force induced reaction method (AFIR) in the global reaction route mapping strategy provided insights into the Zn(OTf)$_2$-mediated hydroarylations and the associated intriguing solvent effects of *t*-BuOH facilitating protodezincation process without a Brønsted acid activator under neutral conditions.
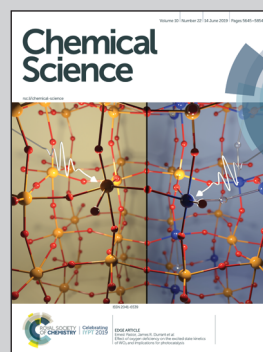
ROYAL SOCIETY OF CHEMISTRY | Celebrating IYPT 2019

rsc.li/chemical-science

Registered charity number: 207890

Zn(OTf)$_2$-mediated annulations of *N*-propargylated tetrahydrocarbolines: divergent synthesis of four distinct alkaloidal scaffolds†

Sadaiwa Yorimoto,[a] Akira Tsubouchi,[a] Haruki Mizoguchi,[b] Hideaki Oikawa, [ID][c] Yoshiaki Tsunekawa,[c] Tomoya Ichino,[c] Satoshi Maeda [ID] *[cd] and Hiroki Oguri [ID] *[a]

Intramolecular hydroarylations of *N*-propargylated tetrahydrocarbolines were efficiently mediated using a unique combination of Zn(OTf)$_2$ with *t*-BuOH under neutral conditions. Use of the artificial force induced reaction method in the global reaction route mapping strategy provided insights into the Zn(OTf)$_2$-mediated hydroarylations and the associated intriguing solvent effects of *t*-BuOH facilitating a protodezincation process without a Brønsted acid activator. We systematically implemented three distinct hydroarylations as well as an unanticipated α-alkenylation of a carbonyl group to obtain the four alkaloidal scaffolds **2–4**, and **18**. Zn(OTf)$_2$-mediated annulation of **1c** proceeded through kinetic formation of the spiroindole **3c** followed by an alkenyl shift and concomitant retro-Mannich-type fragmentation to furnish azepino[4,5-*b*]indole **2** framework. Substituents on substrate **1** in the vicinity of the reaction sites substantially affected the mode of the divergent annulations. Judicious choices of the substituents, solvent and reaction conditions enabled programmable divergent synthesis of the four distinct skeletons.

Introduction

The activation of alkynes with transition metal mediators used as "π-acids" enables efficient carbon–carbon or carbon–heteroatom bond-forming reactions. Whilst various metal catalysts have been reported for the hydroarylation of alkynes,[1] synthetic approaches employing zinc(ɪɪ) reagents for the activation of alkynes currently remain very limited.[2] Herein we report Zn(OTf)$_2$-mediated divergent cyclizations of *N*-propargylated tetrahydrocarbolines **1** towards programmable synthesis of the four distinct skeletons **2–5**, reminiscent of naturally occurring indole alkaloids (Fig. 1a and b). This study provides rare examples of the activation of alkynes with zinc(ɪɪ) reagents in protic solvent (*t*-BuOH) under almost neutral conditions without Brønsted acid promoters. Exploiting the artificial force induced reaction (AFIR) method in the global reaction route
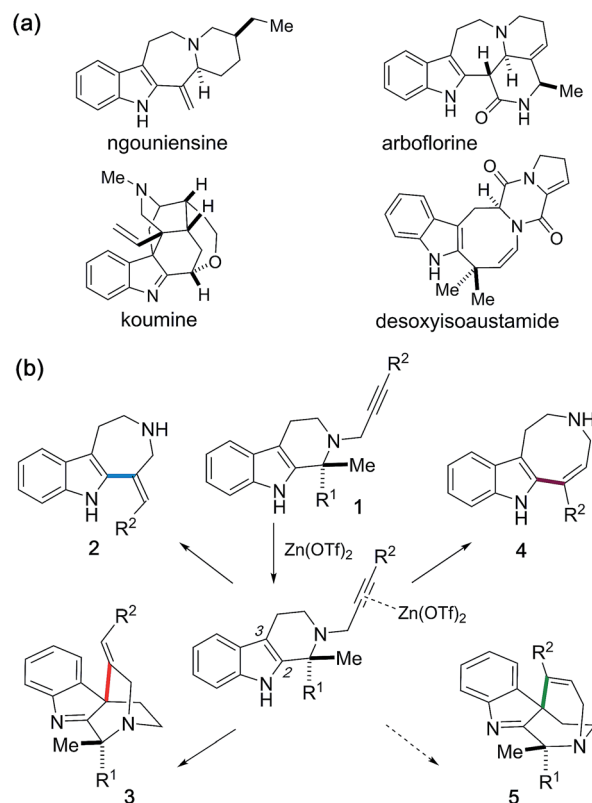
[a]Department of Applied Chemistry, Graduate School of Engineering, Tokyo University of Agriculture and Technology, 2-24-16 Nakacho, Koganei, Tokyo 184-8588, Japan. E-mail: h_oguri@cc.tuat.ac.jp

[b]Graduate School of Natural Science and Technology, Okayama University, 3-1-1 Tsushimanaka, Kita-ku, Okayama 700-8530, Japan

[c]Department of Chemistry, Faculty of Science, Hokkaido University, Kita-ku Kita 10 Jo Nishi 8 Chome, Sapporo 060-0810, Japan. E-mail: smaeda@eis.hokudai.ac.jp

[d]Institute for Chemical Reaction Design and Discovery (WPI-ICReDD), Hokkaido University, Sapporo 001-0021, Japan

Fig. 1 (a) Naturally occurring alkaloids. (b) Zn(OTf)$_2$-mediated divergent cyclizations of **1** for systematic generation of four distinct scaffolds **2–5**.

mapping strategy (GRRM),[3] we postulated that participation of *t*-BuOH as a proton donor dramatically facilitates the proto-dezincation process to promote the zinc(II)-mediated hydro-arylations. Furthermore, divergent annulations to access the four scaffolds **2–5** were systematically implemented *via* appropriate choices of the substituents on **1**, as well as the solvent and reaction conditions.

We incidentally discovered the zinc(II)-mediated ring-expansion reactions of *N*-propargylated tetrahydrocarbolines involving intramolecular hydroarylation of alkynes during the course of our synthetic studies on terpene indole alkaloids.[4] Since the hetero-conjugate addition of **6** to methyl propiolate and subsequent Hofmann elimination *via* the resulting zwit-terionic intermediate smoothly proceeded at room temperature to generate **7**,[4a] we originally aimed to conduct essentially the same conversion employing *N*-propargylated tetrahydrocarbo-line **1a** in place of **6** to afford **7** (Fig. 2a). Contrary to the smooth conversion of **6** (a β-amino acid substructure), the correspond-ing transformation with the sterically more congested **1a** bearing an α, α-disubstituted amino acid moiety resulted in no reaction. To facilitate the initial hetero-conjugate addition of **1a** to methyl propiolate, ZnBr₂ was added as an oxophilic Lewis acid that could activate methyl propiolate through coordination to the ester moiety. Although we failed to achieve the intended conversion leading to **7**, this attempt led to the unexpected discovery of Zn(II)-mediated ring expansion reactions to forge azepino[4,5-*b*]indole **8** and azocino[5,4-*b*]indole **9** scaffolds in modest yields (Fig. 2b). We anticipated that the seven and eight-membered rings **2a** and **4a** could be formed *via* hydroarylation

reactions between the indole C2 position and either the internal or terminal carbon of the alkyne with hydrolytic release of the methyl pyruvate unit. Subsequent hetero-conjugate additions of the resulting secondary amines **2a** and **4a** to methyl propiolate would yield **8** and **9**, respectively.

As a pioneering example of intramolecular hydroarylation employing an indole group, Echavarren reported both cationic Au(I)-catalyzed 7-*exo*-dig (**10** → **11**) and Au(III)-catalyzed 8-*endo*-dig (**10** → **12**) cyclizations (Fig. 3).[5] Van der Eycken devised a regio-controlled annulation (**13** → **14**) employing cationic Au(I) catalyst to construct the functionalized azocino[5,4-*b*] indole scaffold.[6] Recently, Wang and co-workers reported Au(I)-catalyzed cyclizations of **15** having either an internal or terminal alkyne to form azocino[5,4-*b*]indole **16** and spirocyclic scaffold **17**, respectively.[7] Addition of methanesulfonic acid (MsOH) as the Brønsted acid promoter was reported to be essential for complete conversion of **15**. Whilst Au(I)/Au(III)-catalyzed intra-molecular hydroarylations of related indole systems have been developed,[8] there are very few examples of similar conversions employing zinc(II)[9] and other metal promoters.[10] Given the advantages of zinc reagents (*e.g.*, their abundance, low cost, low toxicity, biological relevance, distinct catalytic abilities, and
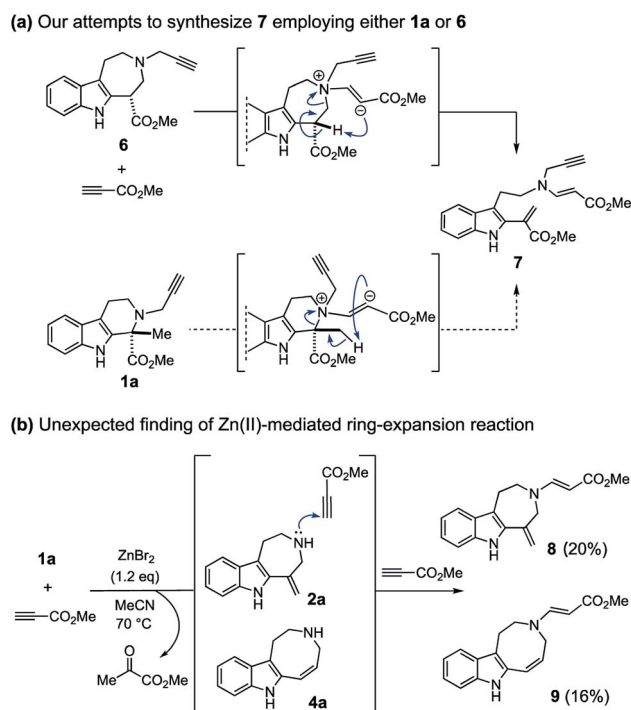

Fig. 2 (a) The reaction of **6**/**1a** with methyl propiolate in the absence of metal promoter. (b) Incidental discovery of the Zn(II)-mediated ring-expansion reactions.
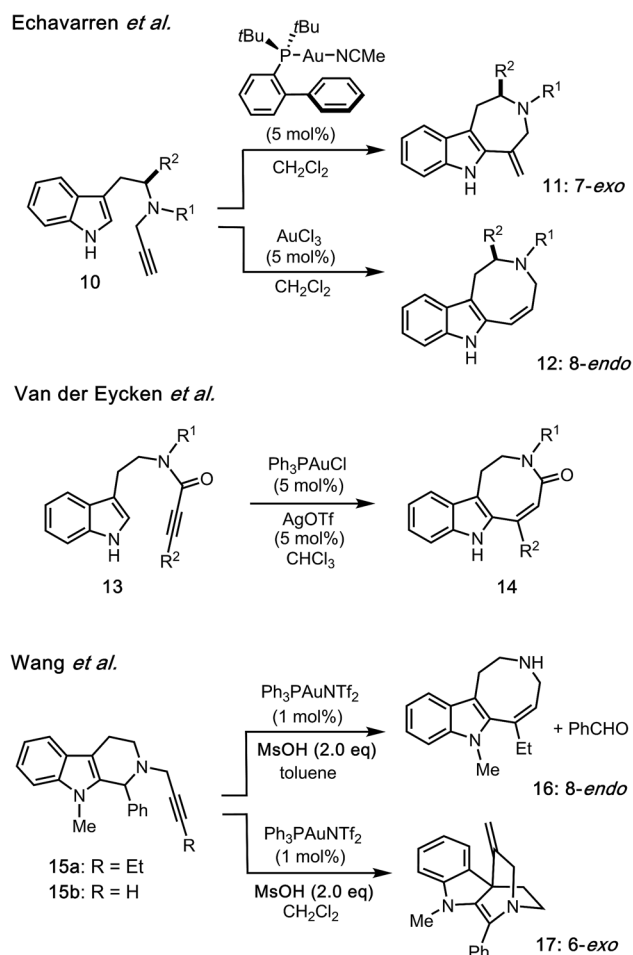

Fig. 3 Au(I)/Au(III)-catalyzed intramolecular hydroarylations of alkynes with indoles.

functional group tolerance), zinc-mediated reactions could provide a sustainable and environmentally benign alternative to the use of more expensive or toxic transition metals.

Results and discussion

Screening of Zn(II)-mediated cyclizations

Intrigued by the unexpected finding shown in Fig. 2b, zinc reagents and solvents were screened to improve the ring-expansion reaction of **1a** to form **2a** (Table 1). The combination of $Zn(OTf)_2$ in *t*-BuOH appeared to be optimal. The cyclizations mediated by $ZnCl_2$, $ZnBr_2$, ZnI_2, and $Zn(OAc)_2$ resulted in poor or moderate conversions (entries 1–4). Other zinc(II) salts composed of counter anions with highly electron-withdrawing properties, such as $Zn(NTf_2)_2$ and $Zn(NO_3)_2$, were slightly less effective compared to $Zn(OTf)_2$ (entries 5–7).

The $Zn(OTf)_2$-mediated hydroarylation of **1a** was greatly affected by the reaction solvent. The use of polar aprotic solvents such as acetonitrile and tetrahydrofuran resulted in decreased yields of **2a** (entries 8–9). In contrast, use of the sterically demanding alcoholic solvent *t*-BuOH dramatically increased the reaction rate (entry 7). The substrate **1a** was completely consumed within 1 hour to afford **2a** in 76% yield as the major product along with formation of byproducts **3a** (13%) and **4a** (6%) bearing spirocyclic and azocino[5,4-*b*]indole scaffolds, respectively. The use of methanol, ethanol, DMF, or DMSO as solvent resulted in poor conversions.

Zn(OTf)₂-mediated cyclization of substrate 1a

Based on the above screening results, we performed $Zn(OTf)_2$-mediated cyclizations under the optimized conditions employing *t*-BuOH as a solvent in the presence of MS4A (Fig. 4). The use of molecular sieves allowed consistent reproduction of the
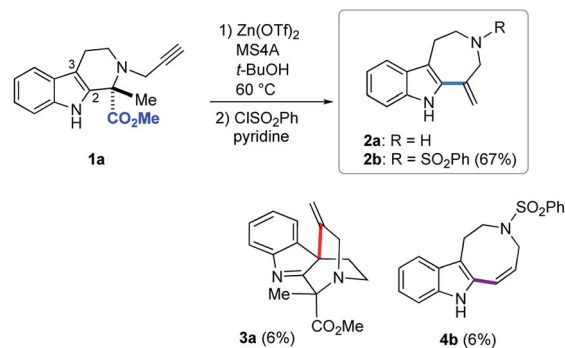
Table 1 Screening of Zn(II) reagents and solvents for the ring-expansion reaction of **1a** to form **2a**[a]

Entry	ZnX₂	Solvent	Time	Yield[b] (%)			Recovery (%)
				2a	**3a**	**4a**	
1	ZnCl₂	*t*-BuOH	24	5	30	22	23
2	ZnBr₂	*t*-BuOH	24	6	35	26	4
3	ZnI₂	*t*-BuOH	24	8	37	19	—
4	Zn(OAc)₂	*t*-BuOH	24	—	—	—	99
5	Zn(NTf₂)₂	*t*-BuOH	24	33	—	6	—
6	Zn(NO₃)₂[b]	*t*-BuOH	24	46	11	20	15
7	**Zn(OTf)₂**	**_t_-BuOH**	**1**	**76**	**13**	**6**	—
8	Zn(OTf)₂	MeCN	6	18	5	2	—
9	Zn(OTf)₂	THF	24	45	6	8	—

[a] All reactions were performed using **1a** (0.2 mmol) and $Zn(OTf)_2$ (0.2 mmol) in 1 mL of each solvent at 60 °C. [b] Determined by ^{1}H-NMR analysis.

Fig. 4 $Zn(OTf)_2$-mediated hydroarylation of **1a**.

experimental results, since $Zn(OTf)_2$-mediated conversions in *t*-BuOH were noticeably affected by trace amounts of water. Due to the practical difficulty of isolating **2a**, isolated yields of the products were reported after benzenesulfonylation of the resultant secondary amino group of **2a**, in which the major product **2b** (67%), along with **4b** (6%) and **3a** (6%), were obtained *via* 7-*exo*, 8-*endo* ring-expansion reactions and spiro-cyclization, respectively. In this paper, we adopted terms, such as 6-*exo*, 7-*exo*, and 8-*endo*, for indication of the formal cyclization modes regardless of the actual reaction mechanisms.

Mechanistic insights into Zn(OTf)₂-mediated hydroarylation

We performed DFT calculations to gain mechanistic insights into the $Zn(OTf)_2$-mediated cyclizations. Stable and transition state (TS) structures were systematically identified using the artificial force induced reaction (AFIR) method implemented in the GRRM program.[3,11,12] All structures were optimized at the ωB97X-D/Def2-SVP level of theory and the solvent effects of *t*-BuOH were evaluated by the solvation model based on density (SMD) method.
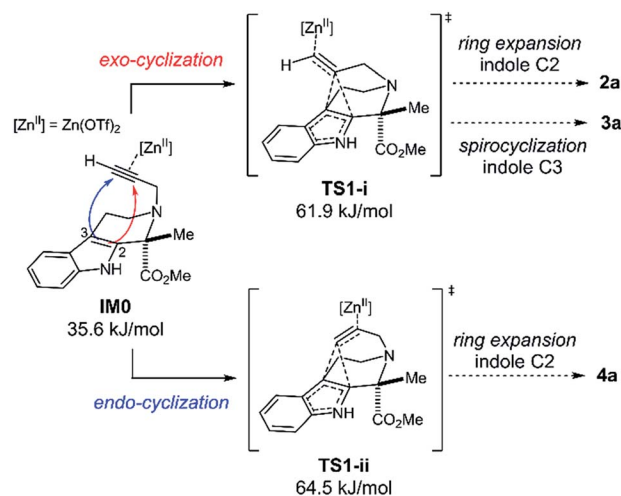

Fig. 5 Two intramolecular cyclization pathways. Gibbs energies ($T = 333.15$ K) relative to the sum of the Gibbs energies for separately calculated **1a** and $Zn(OTf)_2$ are shown in kJ mol^{-1}.
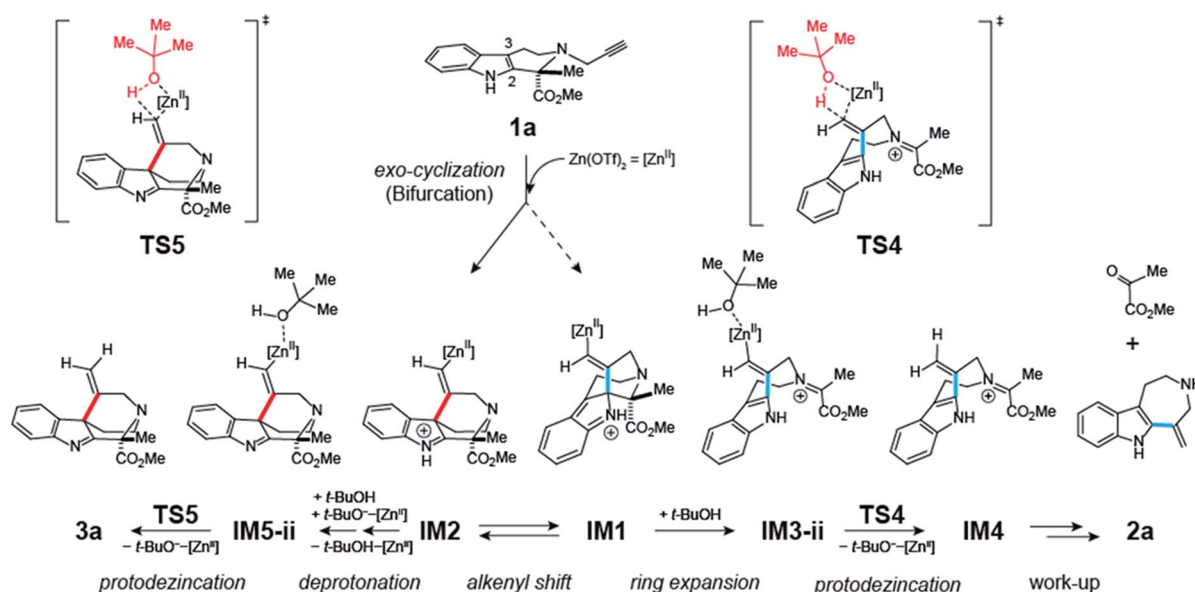
We will discuss the initial *exo-/endo*-cyclization of **1a** (Fig. 5): the *exo*-cyclization affords either **2a** or **3a**, whereas *endo*-cyclization gives **4a**. The propargyl group in **1a** coordinates to Zn(OTf)$_2$ to form the pre-reaction complex **IM0**. A systematic TS structure search identified **TS1-i** and **TS1-ii** as the lowest TS structures for the *exo-* and *endo*-cyclizations, respectively.

In these TS structures, one of the alkynyl-carbon atoms bridges the indole C2 and C3 atoms. Fig. 5 shows that *exo*-cyclization *via* **TS1-i** is kinetically preferred over *endo*-cyclization *via* **TS1-ii**. Our search of the TS structures identified 24 TSs for the *exo*-cyclization and 34 TSs for the *endo*-cyclization reactions (see ESI, Fig. S2†). The Boltzmann distribution of these 58 TSs suggests that the ratio between the number of molecules that undergo *exo-* and *endo*-cyclization is 80.1 : 19.9. Indeed, **4a** was a minor product in our experiment.

In this study, we focused on the fate of molecules that undergo the kinetically preferred *exo*-cyclization reaction. As illustrated in Fig. 6, an intrinsic reaction coordinate (IRC) calculation from **TS1-i** provided **IM1** and **IM2** as the two end-points. **IM2** can isomerize to **IM1** through the relatively low barrier **TS2**. **IM3-ii** is then generated through a C–C bond scission and subsequent solvent coordination. **IM3-ii** could be a resting state, since it has the lowest energy of any structure along this path. **IM3-ii** undergoes protodezincation to yield **IM4** and *t*-BuO$^−$–[Zn^{II}]. **IM4** is expected to be hydrolyzed to **2a** in the workup procedure.[13]

The process which converts **IM2** to **3a** requires *t*-BuO$^−$–[Zn^{II}] released in the protodezincation processes. The *t*-BuO$^−$ part of *t*-BuO$^−$–[Zn^{II}] abstracts a proton from the indole N–H moiety. Then, solvent coordination and subsequent protodezincation afford **3a**. Notably, all obtained paths not involving *t*-BuO$^−$–
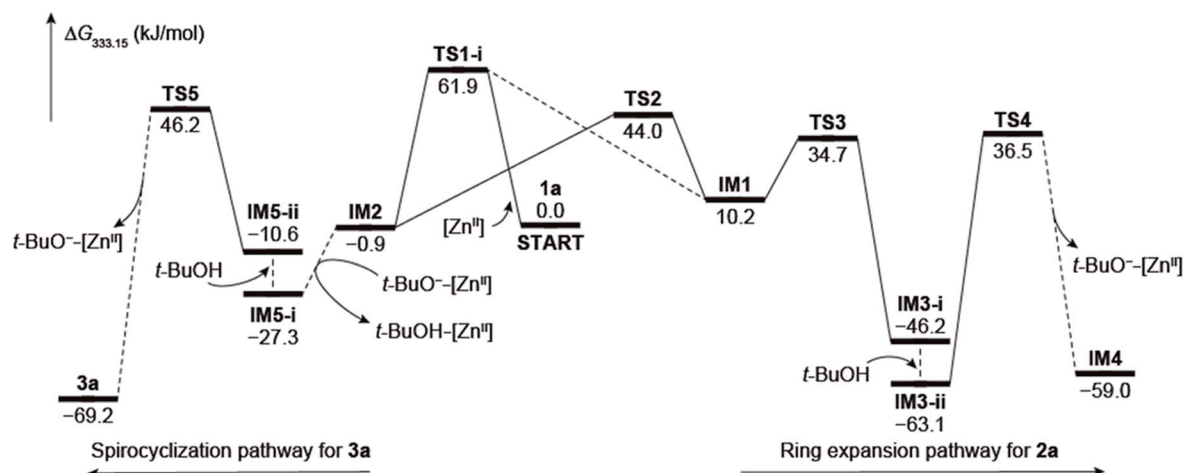

Fig. 6 (a) Reaction mechanism for the two intramolecular cyclization pathways. (b) Energy diagrams for the two cyclization pathways. Gibbs energies (*T* = 333.15 K) relative to the sum of the Gibbs energies for separately calculated **1a** and Zn(OTf)$_2$ are shown in kJ mol$^{−1}$.

[Zn[II]] possess much higher barriers than this path, as shown in Fig. S5 (ESI†).

It was previously suggested that dynamical path bifurcation occurs in the *exo-/endo*-cyclization step of **1a** when the process is catalyzed by an Au catalyst,[7] and thus we searched for the valley–ridge transition (VRT) point[14] along the IRC path from **TS1**. As shown in Fig. S6 (ESI†), the VRT point was identified, indicating that dynamical path bifurcation indeed occurs in the present system. In other words, the elementary process through **TS1** may give not only **IM2**, but also a certain ratio of **IM1**, although quantitative determination of this ratio through extensive MD simulations is beyond the scope of this study.

We conducted a kinetic simulation to illustrate the time evolution of the population of each species, with the initial population comprising exclusively **IM2**. The rate equations shown in ESI† were solved numerically, and the time evolution of the population of each species in 1 hour was computed. Details of this simulation are described in ESI.† Fig. 7 shows the time evolution of the population of intermediates and products. The initial population (**IM2**) decreases within 1 μs, and simultaneously, the population of **IM3-ii** increases. As mentioned above, **IM3-ii** is a resting state and is dominant until around 100 s. Finally, the populations of **IM4** and **3a** increase gradually until 3600 s, to a final ratio of **IM4** : **3a** = 84 : 8, consistent with the experimental yields of **2a** (76%; formed from **IM4**) and **3a** (13%), respectively.

Au(I)/Au(III)-catalyzed hydroarylations of alkynes often necessitate a Brønsted acid activator such as methanesulfonic acid (Fig. 3).[7] In sharp contrast, reaction conditions employing the unique combination of Zn(OTf)$_2$ and *t*-BuOH significantly accelerated the intramolecular cyclizations, facilitating the corresponding protodemetallation process under almost neutral conditions. Based on this calculation, the corresponding protodezincation reaction (**IM3-ii** → **IM4**) has been demonstrated to have the largest activation energy and thus is the rate-determining step. This computational analysis offers hitherto unmarked mechanistic insights into the participation of *t*-BuOH in Zn(II)-mediated hydroarylation reactions *via* transition states (**TS4** and **TS5**) and may provide a rational explanation for our experimental findings of the intriguing solvent effects resulting in substantial rate accelerations.
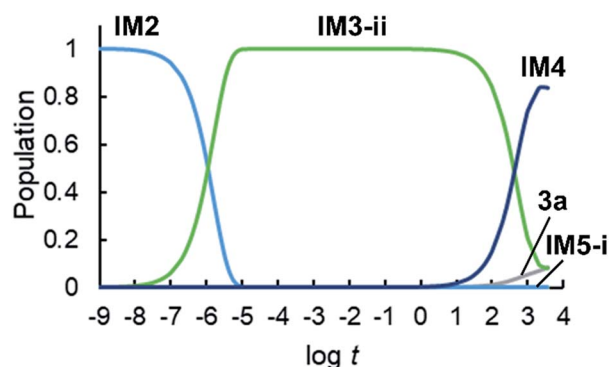
We verified the involvement of the cationic species **IM3-ii**, a putative resting state, in the reaction pathway leading to **2a** by conducting the Zn(OTf)$_2$-mediated ring-expansion reaction in the presence of Et$_3$SiH (Fig. 8). This attempt resulted in the isolation of the corresponding product **2d** (13% yield) *via* reduction of the iminium cation corresponding to **IM3-ii** along with **2b** (67%). Despite the modest yield of **2d**, this experimental result is consistent with the proposed mechanism.

Zn(OTf)$_2$-mediated annulations with distinct substrates

Next, the substrates were modified (Fig. 9) not only to explore the scope of potential substrates but also to change the annulation modes for gaining divergent access to distinct skeletons. To this end, we designed and synthesized substrate **1b**, which bears a benzyl amide group in place of the methyl ester substituent of **1a**. Zn(OTf)$_2$-mediated cyclization of **1b** at 60 °C in *t*-BuOH furnished **3b** with a quaternary carbon center *via* 6-*exo* dearomatizing spirocyclization in 60% yield as the major product. This reaction is in sharp contrast to the conversion of substrate **1a** to **2b** *via* 7-*exo* cyclization shown in Fig. 4. Annulations of **1c** possessing a *gem*-dimethyl moiety resulted in the formation of approximately equimolar amounts of **2b** (44%) and **3c** (44%). The relative stereochemistries of the spirocyclic products **3a–c** were determined based on either NOE or X-ray analysis (Fig. 9).[15]

The Zn(OTf)$_2$-mediated annulation of **1c** provided a **3c** : **2a** product ratio that reversed over time (Fig. S1, see, ESI†). The spirocyclic product **3c** was the major product at the beginning of the reaction but decreased with time as the yield of **2a** gradually increased and eventually exceeded that of **3c** after approximately 80 h.

Zn(OTf)$_2$-mediated conversion of spiroindole 3 to the azepino [4,5-*b*]indole scaffold 2

Given these experimental results, we hypothesized that the Zn(OTf)$_2$-mediated hydroarylations of **1a–c** likely involve the kinetically-controlled formation of spirocyclic products (**3a–c**) and subsequent rearrangement of the alkenyl group concomitant with fragmentation leading to azepino[4,5-*b*]indole **2a** as a thermodynamic product. In fact, treatment of **3c** with
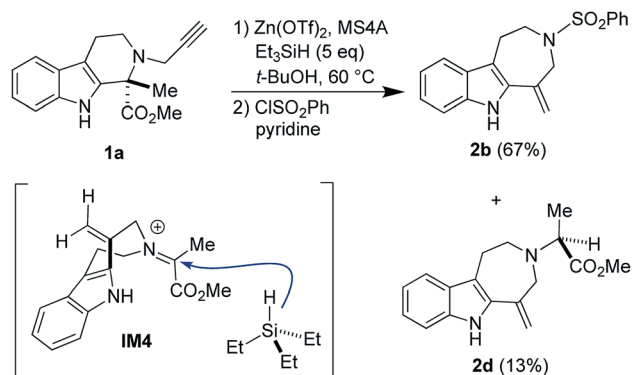

Fig. 7 Time evolution of the population of intermediates and products in 3600 s.

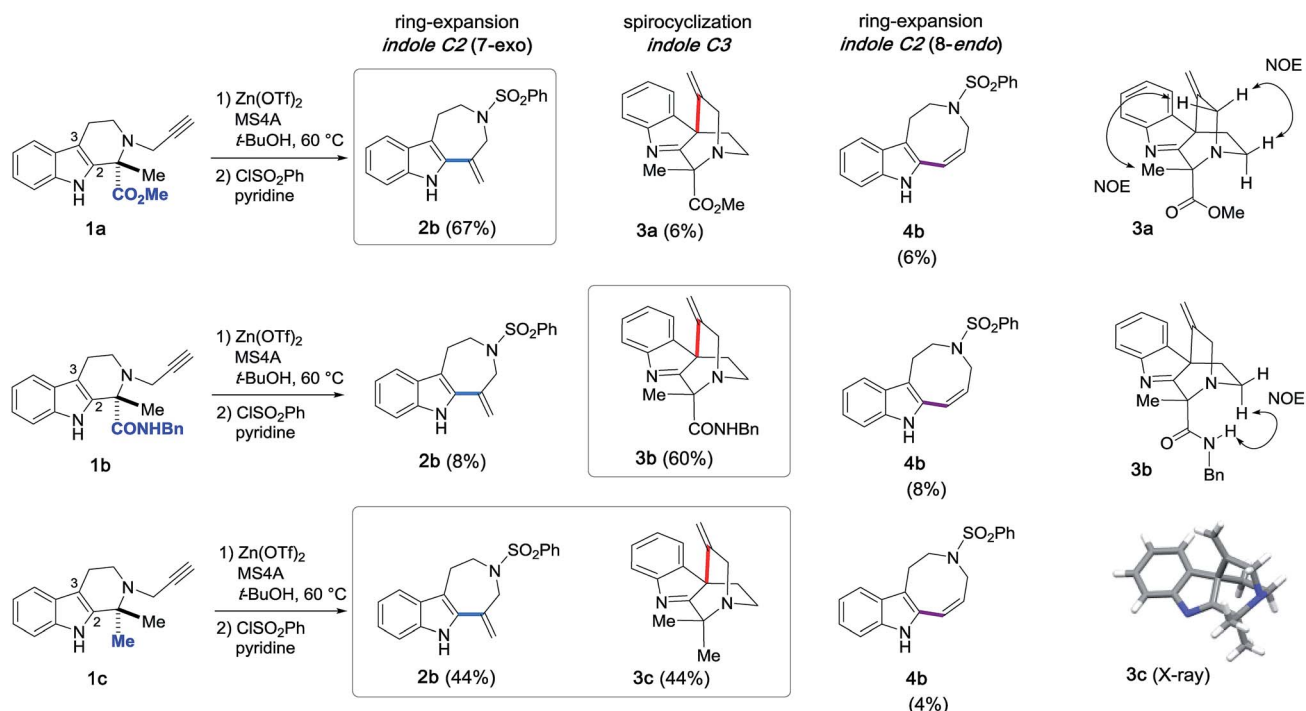Fig. 8 An attempt to trap the intermediate **IM4** to form **2d**.

Fig. 9 Zn(OTf)$_2$-mediated intramolecular hydroarylations of alkynes with indoles and structural elucidation of the spirocyclized products **3a–c**.

Zn(OTf)$_2$ at elevated temperature (100 °C) in 2-BuOH resulted in the expected efficient conversion of **3c** into **2a**, and subsequent benzenesulfonylation of the resulting **2a** afforded **2b** in high yield (93%) (Fig. 10). This experimental result clearly indicated the conversion of **3c** to **2a** under high temperature conditions.

Based on these experimental findings, we propose the reaction mechanism shown in Fig. 10. Activation of an imine group by Zn(OTf)$_2$ could facilitate an alkenyl shift from the C3 to the C2 position to generate a tertiary cation at the benzylic C3 position (**IM6** → **IM7**). Retro-Mannich-type reaction of the tertiary cation **IM7** would entail ring-cleavage and formation of iminium cation intermediate **IM8** and regeneration of the indole system. Hydrolysis of the resulting iminium cation **IM8** would liberate secondary amine **2a** and acetone, followed by sulfonylation of **2a** to provide **2b**. It is worth noting that to our knowledge, there is no previous report of the unexpected and highly efficient conversion of spiroindole **3** to the azepino[4,5-*b*]indole scaffold **2** upon the activation with Lewis acid promoters, whilst the Au(I)/Au(III)-catalyzed related intramolecular hydroarylations of indole and alkyne linear substrates have been reported.[7]

A similar conversion of the spirocycle **3a** bearing a methylester group proceeded, presumably *via* an alkenyl shift followed by ring-cleavage, to afford **2b** in 45% isolated yield after sulfonylation of the resultant **2a**. In contrast, the reaction of **3b**, which bears a benzyl amide group, resulted in poor conversion to form **2b** in 6% yield over two steps and recovery of the substrate **3b** (55%). These experimental results imply that the substituent (R^1: Me, CO$_2$Me, and CONHBn) in the vicinity of the bridgehead aliphatic nitrogen can greatly influence the migration ability of the alkenyl group for the spirocyclic substrates **3a–c**, thereby changing the product distribution between the azepino[4,5-*b*]indole **2** and spirocyclic **3** scaffolds.
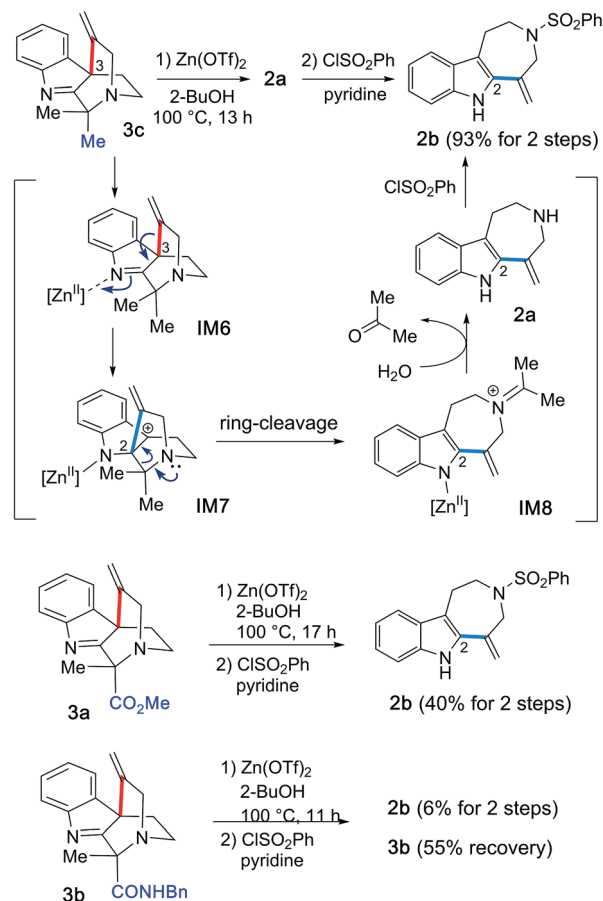

Fig. 10 Conversions of **3a–c** to **2b** and a mechanistic rationale.

Attempts to control product distribution by the choice of reaction solvent

We changed the reaction solvent in an attempt to improve the selectivities of the Zn(OTf)$_2$-mediated cyclizations of **1c** leading to **2a** and **3c** (Table 2). Use of either a secondary alcohol (2-BuOH/i-PrOH) or ethanol instead of t-BuOH provided the spirocyclic product **3c** as the major product (entries 1–4), whereas the use of methanol substantially impeded the conversion (entry 5). In contrast, the use of polar aprotic solvents, such as acetonitrile or THF, enabled preferential formation of **2a** as the major product in good yield (entries 6 and 7). Thus, appropriate choice of the reaction solvent allowed the divergent synthesis of azepino[4,5-b] indole **2a** and spirocycle **3c** in practical yields. The Zn(OTf)$_2$-mediated conversion of substrates **1a–c** bearing a terminal alkyne was accompanied by the competing formation of azocino[5,4-b]indole scaffold **4a**, giving the corresponding **4a** and **4b** in less than 10% yield.

Regio-controlled hydroarylation to form the azocino[5,4-b] indole scaffold

Whilst formation of the azocino[5,4-b]indole scaffold **4a** was a minor pathway for substrates **1a–c** bearing a terminal alkyne, changing the terminal alkyne into an internal alkyne (**1a** → **1d**) reversed the cyclization mode to afford **4c** as the major product via 8-endo-dig mode with loss of a methyl pyruvate unit (Fig. 11). Subsequent acetylation afforded crystalline **4d** in 56% yield (2 steps), and the structure of **4d** was unambiguously confirmed by X-ray analysis. Similarly, Zn(OTf)$_2$-mediated 8-endo cyclization of **1e**, followed by acetylation, provided **4d** in good yield (91% over 2 steps).
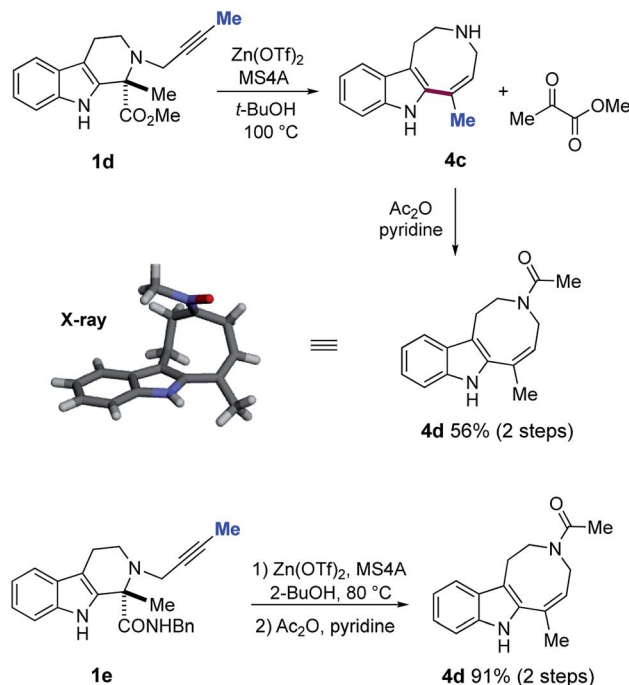

Fig. 11 Zn(OTf)$_2$-mediated ring expansion reaction of **1d–e** and subsequent acetylation to form **4d** and X-ray analysis of **4d**.

Substrate design for 7-endo cyclization and the unexpected α-alkenylation of a carbonyl group

We integrated the computational and experimental insights obtained throughout this study to investigate the remaining 7-endo cyclization between the indole C3 position and the distal alkynyl carbon to construct the spirocyclic scaffold **5** (Fig. 1b). To this end, we designed the new substrate **1f** possessing both an amide moiety and an α-proton at the carbonyl group (Fig. 12a). We anticipated that kinetically-favored spirocyclization at the indole C3 position would form the iminium cation **IM9** stabilized by hydrogen bonding between the bridgehead nitrogen and the amide N–H proton.

More importantly, installation of an α-proton would facilitate conversion of the iminium cation into the relatively stable enamine (**IM9** → **IM10**) by preventing the competitive alkenyl shift to form intermediate **IM11** for the 8-endo cyclization, which leads to undesired product **4c** via **IM12**.

Contrary to expectation, Zn(OTf)$_2$-mediated cyclization of **1f** in 2-BuOH did not afford the desired 7-endo product **5f**; rather, the 8-endo product **4d** was obtained in 61% yield after acetylation (Fig. 12b). Nonetheless, changing the solvent from 2-BuOH to 1,2-dichloroethane led to unanticipated results. Treatment of **1f** in 1,2-dichloroethane at 100 °C enabled the intriguing Zn(OTf)$_2$-mediated α-alkenylation of the carbonyl group to afford the tetracyclic scaffold **18** containing a quaternary carbon center and a trisubstituted alkene, albeit in 14% yield.[16] Presumably, replacement of the protic solvent (2-BuOH) with the hydrophobic solvent (1,2-dichloroethane) played a crucial role in facilitating Zn(OTf)$_2$-mediated enolization and α-alkenylation reactions which led to **18**. Thus, three distinct modes of

Table 2 Solvent effects for the Zn(OTf)$_2$-mediated conversion of **1c** into **2a** and **3c**[a]

Entry	Solvent	Time	2a	3c	4a	Recovery (%)	2a : 3c
1	t-BuOH	24	45	55	5	—	45 : 55
2	2-BuOH	8	25	**70**	5	—	26 : 74
3	i-PrOH	8	23	**68**	5	—	25 : 75
4	EtOH	24	31	63	5	—	33 : 67
5	MeOH	24	13	40	3	37	25 : 75
6	CH$_3$CN	8	**84**	7	7	2	**92 : 8**
7	THF	24	**80**	6	7	6	**93 : 7**

[a] All reactions were performed using **1c** (0.2 mmol) and Zn(OTf)$_2$ (0.2 mmol) in 1 mL of each solvent at 60 °C. [b] Determined by ^{1}H-NMR analysis.
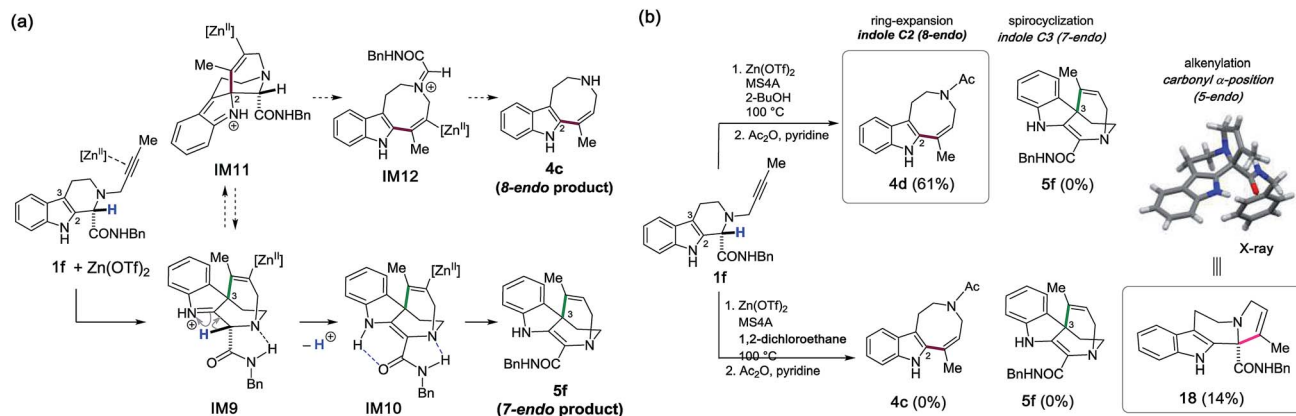
Fig. 12   (a) A strategy for the 7-endo cyclization reaction to form 5f. (b) Zn(OTf)$_2$-mediated cyclizations with substrate 1f.

intramolecular hydroarylations between the indole C2/C3 positions and the internal/distal alkenyl carbons, as well as the unexpected α-alkenylation of the carbonyl group, were systematically realized by employing Zn(OTf)$_2$ as a versatile "π-acid" mediator. A divergent synthetic process was developed in a programmable manner by the rational choice of substituents in the vicinity of the reaction sites, as well as of the solvents and reaction conditions.

Experimental section

All reactions were performed under a nitrogen atmosphere unless otherwise noted. Microwave reactions were performed using a Biotage® Initiator. Reactions were monitored by thin layer chromatography using Merck Millipore TLC Silica gel F254 plates (0.25 mm), which were visualized using UV light, phosphomolybdic acid (PMA) stain, PMS stain and p-anisaldehyde stain. Flash column chromatography was performed using Kanto Silica Gel 60N and Wako Alumina, Activated. The medium pressure liquid chromatography (MPLC) purifications were performed on a YAMAZEN YFLC-AI-580 and Biotage® Isolera. NMR spectra were recorded on JEOL ECA 500 (^{1}H/500 MHz, ^{13}C/125 MHz) and JEOL ECA 400 (^{1}H/400 MHz, ^{13}C/100 MHz) spectrometers. Chemical shifts (δ) were quoted in parts per million (ppm) from chloroform, acetonitrile, and dimethyl sulfoxide as an internal standard of 7.26, 1.94, 2.50 and 77.16, 1.32, 39.52 for ^{1}H and ^{13}C-NMR, respectively. Data for ^{1}H NMR were reported as follows: chemical shift (number of hydrogen, multiplicity, coupling constant). Multiplicity was abbreviated as follows: s (singlet), d (doublet), t (triplet), q (quartet), quin (quintet), m (multiplet), br (broad). ESI-Mass spectra were recorded on Bruker Daltonics microTOF-QII.

Materials

Solvents used for the Zn(OTf)$_2$-promoted reaction were dried and stored over activated molecular sieves 4A. Zn(OTf)$_2$ was purchased from Tokyo Chemical Industry Co., Ltd. (TCI) and used as received. The substrates 1a–f were prepared from commercially available tryptamine hydrochloride (see ESI†).

General procedure for Zn(OTf)$_2$-promoted reaction of N-propargylated tetrahydrocarbolines 1

All reactions were carried out using 1.00 mmol of 1. A solution (0.2 M) of Zn(OTf)$_2$ in t-BuOH was prepared prior to use as follows. Zn(OTf)$_2$ (436 mg, 1.20 mmol) and t-BuOH (6 mL) were mixed in a Biotage microwave vial. The vial was sealed with a Teflon septum lined cap, and the mixture was then heated for 5 min at 100 °C under microwave irradiation to give a homogenous clear solution.

Finely powdered molecular sieves 4A (200 mg) were placed in a microwave vial and dried by heating with a heat gun in vacuo. The t-BuOH solution of Zn(OTf)$_2$ (0.2 M, 5 mL, 1.00 mmol) prepared as mentioned above and compound 1 (1.00 mmol) were successively added. The vial was then sealed with a Teflon septum lined cap. The mixture was stirred for 1 h at room temperature and then heated at 60 °C for appropriate time. After being cooled to room temperature, EtOAc (1 mL) and a saturated aqueous solution (1 mL) of the Rochelle salt were added at 0 °C. The mixture was stirred at 0 °C for 1 h and insoluble materials were filtered off and washed with EtOAc (50 mL) and H$_2$O (5 mL). The organic layer was separated and washed with a saturated aqueous solution (10 mL) of NaHCO$_3$. The aqueous layer was extracted with EtOAc (50 mL × 2). Combined organic extracts were dried over Na$_2$SO$_4$ and concentrated under reduced pressure to give a crude mixture of products 2, 3, and 4.

The products 2 and 4 were isolated after sulfonylation as follows. The crude mixture was dissolved in pyridine (5 mL) and then treated with benzenesulfonyl chloride (0.640 mL, 5.00 mmol) at 0 °C. After being stirred for 10 min at 0 °C and then 30 min at room temperature, the reaction was quenched by addition of a saturated aqueous solution of NaHCO$_3$ at 0 °C. The resulting mixture was extracted with EtOAc (100 mL) and washed with a saturated aqueous solution of NaHCO$_3$ (10 mL) and H$_2$O (10 mL). Combined aqueous layers were extracted with EtOAc (100 mL). Combined organic extracts were washed with brine and dried over Na$_2$SO$_4$. After filtration and concentration in vacuo, the products were isolated by column chromatography.

Reaction of 1a bearing a methylester group

According to the general procedure, $Zn(OTf)_2$-promoted reaction of **1a** (283 mg, 1.00 mmol) was carried out. The resulting mixture was purified by silica gel column chromatography (CH_2Cl_2/MeCN) to give a fraction containing **2b** and **4b** (248 mg, 0.733 mmol, 73%, **2b** : **4b** = 92 : 8) as well as a fraction containing **3a**. The fraction mainly composed of **3a** was further purified by alumina column chromatography (CH_2Cl_2) to give **3a** (17 mg, 0.0602 mmol, 6%). Whilst the mixture composed of **2b** and **4b** was separable via repetitive column chromatography, it caused significant decrease in isolated yields. **2b**: R_f = 0.30 (CH_2Cl_2); ^1H NMR (500 MHz, CDCl$_3$) δ 7.82 (1H, br s), 7.78–7.76 (2H, m), 7.47–7.44 (2H, m), 7.38–7.35 (2H, m), 7.27–7.25 (1H, m), 7.20–7.11 (1H, m), 7.10–7.07 (1H, m), 5.24 (1H, s), 5.22 (1H, s), 4.34 (2H, s), 3.74 (2H, t, J = 5.7 Hz), 3.06 (2H, t, J = 5.7 Hz); ^{13}C NMR (125 MHz, CDCl$_3$) δ 139.9, 137.5, 136.0, 133.1, 132.4, 128.9, 128.4, 127.1, 123.2, 119.7, 118.5, 113.1, 111.8, 110.8, 52.7, 49.1, 24.2. HRMS (ESI, m/z): calcd for $C_{19}H_{18}KN_2O_2S$ [M + K]$^+$ 377.0721, found 377.0721. **3a**: R_f = 0.30 (CH_2Cl_2–MeCN = 1 : 2); ^1H NMR (500 MHz, CDCl$_3$): δ 7.74 (1H, d, J = 8.6 Hz), 7.42–7.38 (2H, m), 7.21 (1H, t, J = 7.5 Hz), 4.81–4.80 (1H, m), 4.72–4.71 (1H, m), 3.94 (1H, br d, J = 18.1 Hz), 3.84 (3H, s), 3.74 (1H, ddd, J = 18.1, 2.3, 2.3 Hz), 3.22 (1H, ddd, J = 14.8, 10.2, 5.4 Hz), 3.07–3.00 (1H, m), 2.31 (1H, ddd, J = 12.3, 10.6, 5.2 Hz), 1.77 (3H, s), 1.63 (1H, ddd, J = 12.3, 10.6, 5.2 Hz); ^{13}C NMR (125 MHz, CDCl$_3$): δ 185.4, 171.4, 157.1, 143.9, 137.4, 128.5, 125.5, 124.3, 121.8, 106.4, 67.8, 59.2, 53.4, 51.1, 46.8, 27.0, 23.7; HRMS (ESI, m/z): calcd for $C_{17}H_{19}N_2O_2$ [M + H]$^+$ 283.1441, found 283.1466. **4b**: R_f = 0.28 (CH_2Cl_2); ^1H NMR (500 MHz, CDCl$_3$): δ 7.65–7.64 (2H, m), 7.62 (1H, br s), 7.47–7.42 (2H, m), 7.35–7.32 (2H, m), 7.25 (1H, d, J = 8.6 Hz), 7.19–7.15 (1H, m), 7.09 (1H, t, J = 7.4 Hz), 6.49 (1H, d, J = 11.5 Hz), 5.85 (1H, dt, J = 11.5, 6.6 Hz), 4.00 (2H, d, J = 6.9 Hz), 3.60–3.58 (2H, m), 3.00–2.97 (2H, m); ^{13}C NMR (125 MHz, CDCl$_3$): δ 140.1, 136.1, 132.2, 131.6, 128.9, 128.1, 127.4, 127.0, 123.2, 122.8, 119.8, 118.3, 112.4, 110.9, 46.3, 46.1, 24.4; HRMS (ESI, m/z): calcd for $C_{19}H_{18}N_2O_2S$ [M + H]$^+$ 339.1162, found 339.1166.

Reaction of 1b bearing a benzylamide group

According to the general procedure, $Zn(OTf)_2$-promoted reaction of **1b** (357 mg, 1.00 mmol) was carried out. The resulting crude mixture was purified by silica gel column chromatography (CH_2Cl_2/MeCN) to give a mixture of **2b** and **4b** (50.4 mg, 0.145 mmol, 15%; **2b** : **4b** = 1 : 1) as well as **3b** (213 mg, 0.596 mmol, 60%). **3b**: R_f = 0.31 (EtOAc–MeOH = 10 : 1); ^1H NMR (500 MHz, CD$_3$CN): δ 8.19 (1H, t, J = 5.5 Hz), 7.68 (1H, d, J = 8.0 Hz), 7.46 (1H, d, J = 7.5 Hz), 7.34–7.22 (7H, m), 4.78–4.75 (2H, m), 4.48–4.38 (2H, m), 3.90 (1H, br d, J = 17.8 Hz), 3.70 (1H, br d, J = 17.8 Hz), 3.16 (1H, ddd, J = 14.3, 10.3, 4.0 Hz), 2.90–2.82 (1H, m), 2.37–2.30 (1H, m), 1.61 (3H, s), 1.31 (1H, ddd, J = 12.3, 10.6, 4.0 Hz); ^{13}C NMR (125 MHz, CD$_3$CN): δ 189.5, 172.4, 157.3, 144.5, 139.7, 138.6, 129.6, 129.2, 128.21, 128.17, 126.7, 125.5, 122.2, 106.5, 68.4, 60.8, 51.1, 47.3, 43.8, 29.4, 26.9; HRMS (ESI, m/z): calcd for $C_{23}H_{24}N_3O$ [M + H]$^+$ 358.1914, found 358.1943.

Reaction of 1c bearing a gem-dimethyl group

According to the general procedure, $Zn(OTf)_2$-promoted reaction of **1c** (238 mg, 0.999 mmol) was carried out. The resulting crude mixture was purified by silica gel column chromatography (CH_2Cl_2/MeCN) to give a fraction containing **2b** and **4b** (163 mg, 0.482 mmol, 48%; **2b** : **4b** = 91 : 9) as well as a fraction containing **3c**. The fraction mainly composed of **3c** was further purified by alumina column chromatography (CH_2Cl_2) to afford **3c** (104 mg, 0.436 mmol, 44%). **3c**: R_f = 0.11 (CH_2Cl_2–MeCN = 1 : 1); ^1H NMR (500 MHz, CDCl$_3$): δ 7.61 (1H, d, J = 8.0 Hz), 7.36 (1H, d, J = 7.5 Hz), 7.33 (1H, dd, J = 8.0, 7.5 Hz), 7.20 (1H, dd, J = 8.0, 7.5 Hz), 4.81–4.80 (1H, m), 4.70–4.67 (1H, m), 3.92 (1H, br d, J = 18.1 Hz), 3.63 (1H, br d, J = 18.1 Hz), 3.37–3.31 (1H, m), 3.05–2.98 (1H, m), 2.32–2.27 (1H, m), 1.57 (3H, s), 1.53–1.46 (1H, m), 1.49 (3H, s); ^{13}C NMR (125 MHz, CDCl$_3$): δ 192.9, 157.1, 143.7, 137.8, 128.2, 124.9, 124.2, 121.0, 105.8, 59.4, 58.6, 52.4, 44.4, 29.6, 26.4, 26.1; HRMS (ESI, m/z): calcd for $C_{16}H_{19}N_2$ [M + H]$^+$ 239.1543, found 239.1548.

Reaction of 1d and 1e bearing an internal alkyne

Reaction of 1d. According to the general procedure, $Zn(OTf)_2$-promoted reaction of **1d** (297 mg, 1.00 mmol) was carried out at 100 °C. The resulting reaction mixture containing **4c** was acetylated by addition of acetic anhydride (0.473 mL, 5.00 mmol) in pyridine (5 mL) at 0 °C. After being stirred at room temperature, the reaction mixture was quenched by addition of a saturated aqueous solution of NaHCO$_3$ at 0 °C. The resultant mixture was extracted with EtOAc (100 mL) and washed with a saturated aqueous solution of NaHCO$_3$ (10 mL) and H$_2$O (10 mL). Combined aqueous layers were extracted with EtOAc (100 mL). Combined organic extracts were washed with brine and dried over Na$_2$SO$_4$. After filtration and concentration, the residue was purified by silica gel column chromatography (CH_2Cl_2/EtOAc, EtOAc, followed by EtOAc/MeOH) to afford **4d** (143 mg, 0.562 mmol, 56% for 2 steps). **4d** (60 : 40 mixture of rotamers): R_f = 0.29 (CH_2Cl_2–EtOAc = 1 : 1); ^1H NMR (500 MHz, DMSO-d_6, 90 °C): δ 10.7 (1H, br s), 7.52 (1H, br d, J = 7.5 Hz), 7.34 (1H, br d, J = 8.0 Hz), 7.11–7.08 (1H, m), 7.04–6.97 (1H, br m), 5.86–5.80 (0.40H, m), 5.80–5.74 (0.60H, m), 3.83 (0.80H, m), 3.80 (1.20H, m), 3.55 (0.80H, m), 3.46 (1.20H, m), 2.91 (1.20H, m), 2.82 (0.80H, m), 2.16 (1.20H, br s), 2.11 (1.80H, br s), 2.01 (1.20H, br s), 1.67 (1.80H, br s); ^{13}C NMR (125 MHz, DMSO-d_6, 90 °C): δ 169.5, 169.0, 136.9, 136.8, 136.0, 135.1, 131.1, 129.4, 129.1, 128.6, 128.0, 125.8, 125.1, 123.8, 121.9, 119.1, 118.5, 118.2, 111.9, 111.5, 110.4, 55.2, 47.7, 47.6, 45.7, 42.7, 25.3, 24.7, 23.3, 21.7; HRMS (ESI, m/z): calcd for $C_{16}H_{19}N_2O$ [M + H]$^+$ 255.1492, found 255.1494.

Reaction of 1e. According to the general procedure except for changing the solvent from t-BuOH to 2-BuOH, $Zn(OTf)_2$-promoted reaction of **1e** (371 mg, 1.00 mmol) was carried out at 80 °C for 44 h. The resulting crude reaction mixture containing **4c** was acetylated by addition of acetic anhydride (0.473 mL, 5.00 mmol) in pyridine (5 mL) at 0 °C. After being stirred at room temperature, essentially identical workup protocol as described above was applied to give **4d** (232 mg, 0.912 mmol, 91%).

Reaction of 1f. According to the general procedure, a solution (0.2 M) of Zn(OTf)$_2$ (147 mg, 0.405 mmol) in 1,2-dichloroethane (2.0 mL) was prepared in a Biotage microwave vial prior to use. To this was added finely powdered molecular sieves 4A (45.1 mg) which was preactivated by heating with a heating gun *in vacuo* and **1f** (73.0 mg, 0.204 mmol). The vial was then sealed with a Teflon septum lined cap. The mixture was stirred at 30 °C for 1 h and then heated at 100 °C for 4 d. After being cooled to room temperature, the reaction mixture was worked-up in a similar manner to the general procedure. The resulting crude reaction mixture was acetylated by addition of acetic anhydride (0.100 mL, 1.06 mmol) in pyridine (1 mL) at 0 °C. After being stirred at room temperature for 10 min, essentially identical workup protocol as described above was applied to give a crude mixture. This was purified by PTLC (hexane–EtOAc and then CH$_2$Cl$_2$–MeCN) to afford **18** (10.4 mg, 0.0291 mmol, 14%). **18**: R_f = 0.39 (Hexane–EtOAc = 2 : 1); ^{1}H NMR (400 MHz, CDCl$_3$): δ 9.09 (1H, s), 8.43 (1H, t, J = 5.7 Hz), 7.50 (1H, d, J = 7.3 Hz), 7.38 (1H, d, J = 8.2 Hz), 7.35–7.22 (5H, m), 7.16 (1H, ddd, J = 8.1, 6.9, 0.9 Hz), 7.10–7.06 (1H, m), 5.50–5.48 (1H, m), 4.50 (1H, dd, J = 15.1, 6.4 Hz), 4.41 (1H, dd, J = 15.1, 6.0 Hz), 3.81–3.78 (2H, m), 3.33–3.25 (1H, m), 3.08–2.98 (2H, m), 2.60–2.50 (1H, m), 2.01–1.99 (3H, m); ^{13}C NMR (100 MHz, CDCl$_3$): δ 172.3, 140.0, 138.6, 136.5, 133.7, 128.8, 127.5, 126.8, 123.9, 121.9, 119.3, 118.4, 111.6, 109.1, 74.4, 55.4, 45.3, 43.1, 16.8, 14.0; HRMS (ESI, m/z): calcd for C$_{23}$H$_{24}$N$_3$O [M + H]$^+$ 358.1914, found 358.1912.

According to the above procedure except for changing the solvent from 1,2-dichloroethane to 2-BuOH, Zn(OTf)$_2$-promoted reaction of **1f** (72.0 mg, 0.201 mmol) was carried out at 100 °C for 24 h. The resulting crude reaction mixture containing **4c** was treated with acetic anhydride (0.473 mL, 5.00 mmol) in pyridine (5 mL) at 0 °C. After being stirred at room temperature, essentially identical workup protocol as described above was applied to give **4d** (31.0 mg, 0.112 mmol, 61%).

Trapping of iminium cation IM4 *via* reduction with Et$_3$SiH

Finely powdered molecular sieves 4A (400 mg) were placed in a microwave vial and dried by heating with a heat gun *in vacuo*. The *t*-BuOH solution of Zn(OTf)$_2$ (0.2 M, 10 mL, 2.00 mmol) prepared as described above, the compound **1a** (565 mg, 2.00 mmol), and triethylsilane (1.59 mL, 10.0 mmol) were successively added. The vial was sealed with a Teflon septum lined cap and the mixture was stirred at 30 °C for 1 h. The resulting mixture was further heated at 60 °C for 3 h. After being cooled to rt, the reaction mixture was diluted with toluene (10 mL) and concentrated to one fifth of its initial volume under reduced pressure. The residue was diluted with EtOAc (20 mL) and then treated with a saturated aqueous solution (10 mL) of the Rochelle salt at 0 °C. The mixture was vigorously stirred at 0 °C for 1 h, and insoluble materials were filtered off and washed with EtOAc (80 mL) and H$_2$O (5 mL). The organic layer was separated and washed with a saturated aqueous solution of NaHCO$_3$ (10 mL × 2). The aqueous layer was extracted with EtOAc (100 mL × 2). Combined organic extracts were washed with brine (10 mL), dried over Na$_2$SO$_4$, filtered and concentrated

under reduced pressure to give a crude mixture of **2a** and **2d**. The resultant mixture was dissolved in pyridine (10 mL) and treated with benzenesulfonyl chloride (1.28 mL, 10.0 mmol) at 0 °C. After being stirred at room temperature, the mixture was treated with a saturated aqueous solution of NaHCO$_3$ (10 mL). The mixture was extracted with EtOAc (100 mL × 3), washed with brine (15 mL), and dried over Na$_2$SO$_4$. After filtration and concentration, the residue was purified by silica gel column chromatography (CH$_2$Cl$_2$/EtOAc/MeOH) to give **2d** (72.2 mg, 0.253 mmol, 13%). The fraction mainly containing **2b** was further purified by passing through a short alumina column (CH$_2$Cl$_2$) to give **2b** (456 mg, 1.35 mmol, 67%). **2d**: R_f = 0.21 (Hex–EtOAc = 2 : 1); ^{1}H NMR (500 MHz, CDCl$_3$): δ 7.97 (1H, s), 7.49 (1H, d, J = 8.0 Hz), 7.28 (1H, d, J = 8.0 Hz), 7.20–7.16 (1H, m), 7.11–7.07 (1H, m), 5.26 (1H, s), 5.07 (1H, s), 3.84 (1H, d, J = 14.9 Hz), 3.74–3.72 (4H, m), 3.67 (1H, q, J = 6.9 Hz), 3.32 (1H, ddd, J = 13.1, 7.9, 4.3 Hz), 3.21 (1H, ddd, J = 13.1, 7.9, 4.3 Hz), 3.05 (1H, ddd, J = 16.6, 7.6, 3.9 Hz), 2.97 (1H, ddd, J = 16.6, 7.6, 3.9 Hz),1.43 (3H, d, J = 7.5 Hz); ^{13}C NMR (125 MHz, CDCl$_3$): δ 174.8, 140.0, 136.0, 134.0, 129.1, 123.0, 119.5, 118.8, 114.6, 111.2, 110.6, 76.9, 60.3, 58.5, 52.5, 51.8, 24.3, 16.7; HRMS (ESI, m/z): calcd for C$_{17}$H$_{21}$N$_2$O$_2$ [M + H]$^+$ 285.1598, found 285.1614.

General procedure for conversion of 3 into 2b

Zn(OTf)$_2$ (72.7 mg, 0.200 mmol) and 2-BuOH (2 mL) was mixed in a Biotage microwave vial. The vial was sealed with a Teflon septum lined cap. The mixture was heated at 100 °C for 5 min to give a homogenous clear solution. After being cooled to rt, compound **3** (0.200 mmol) were added, and the vial was sealed again with a Teflon septum lined cap. The mixture was then heated at 100 °C for appropriate time. After being cooled to room temperature, the reaction mixture was poured into a mixture of EtOAc and a saturated aqueous solution of the Rochelle salt at 0 °C. The resulting mixture was vigorously stirred at 0 °C for 1 h. The organic layer was separated and washed with a saturated aqueous solution of NaHCO$_3$. The aqueous layer was extracted with EtOAc. Combined organic extracts were washed with brine, dried over Na$_2$SO$_4$ and concentrated under reduced pressure. After azeotropic distillation with toluene, the residue was dissolved in pyridine (2 mL) and then treated with benzenesulfonyl chloride (0.128 mL, 1.00 mmol) at 0 °C. After being stirred at room temperature, the resulting mixture was quenched with saturated aqueous solution of NaHCO$_3$ and extracted with EtOAc. Combined organic extracts were washed with brine and dried over Na$_2$SO$_4$. After filtration and concentration under reduced pressure, the residue was purified by silica gel column chromatography (CH$_2$Cl$_2$/MeCN) to give **2b** and **3**.

Reaction of 3a. According to the above procedure, the reaction of **3a** (56.5 mg, 0.200 mmol) with Zn(OTf)$_2$ was conducted to give **2b** (26.8 mg, 79.2 μmol, 40% in 2 steps) along with recovery of **3a** (5.5 mg, 19.5 μmol, 10%).

Reaction of 3b. According to the above procedure, the reaction of **3b** (71.5 mg, 0.200 mmol) with Zn(OTf)$_2$ was conducted to give **2b** (4.1 mg, 12.1 μmol, 6% in 2 steps) along with recovery of **3b** (39.6 mg, 111 μmol, 55%).

Reaction of 3c. According to the above procedure, the reaction of **3c** (47.7 mg, 0.200 mmol) with $Zn(OTf)_2$ was conducted to give **2b** (62.9 mg, 186 μmol, 93% in 2 steps).

Computational session

We have performed an initial reaction path search adopting a simplified model to reduce computational costs. In the model, the benzene ring in the indole moiety was substituted by methyl groups at the C4 and C5 positions. In the initial reaction stage, we focused only on bond reorganizations among four carbon atoms, *i.e.*, two alkynyl carbon atoms in the propargyl moiety and indole C2 and C3 atoms, based on the reaction mechanism proposed by Wang and coworkers.[7] In this stage, the model collision energy parameter γ of the AFIR method was set to 200 kJ mol^{-1}. The subsequent C–C bond fission steps were studied by manually applying the artificial force to specific atom pairs with $\gamma = 100$ kJ mol^{-1}. TSs for the protodezincation steps were searched by shooting *t*-BuOH to **IM3-i** or **IM5-i** from various random mutual positions and directions by the AFIR method with $\gamma = 200$ kJ mol^{-1}, where the OH groups in *t*-BuOH and Zn, and the Zn–bound alkenyl carbon atom in **IM3-i** or **IM5-i** were set as two fragments in the AFIR function. In these search jobs, DFT calculations were carried out at the RI-PBE[17]/def2-SV(P)[18] level implemented in Turbomole v.7.0.1 program.[19]

The AFIR paths obtained in the above calculations were optimized by the locally updated plane (LUP) method[20] to obtain initial structures for TS optimizations. From all optimized TS structures, IRC calculations were performed to see path connections. Harmonic vibrational analysis was carried out at all optimized TS and stable structures. In these jobs, DFT calculations were performed at the B3LYP[21]/Def2SVP level combined with the SMD (*t*-BuOH) method[22] implemented in Gaussian 09 program.[23]

The reaction pathways of **1a** leading to **2a**/**3a** were obtained based on corresponding paths obtained in the simplified model system. Intermediate and TS structures were reoptimized with the ωB97X-D[24]/Def2SVP level with the SMD (*t*-BuOH) method. To identify the lowest conformation at TS, TS conformation sampling was made for intramolecular cyclization and protodezincation steps. The conformation at these TSs were systematically searched by the AFIR method with fixing positions of atoms involved in each bond reorganization, at the PBEPBE/Def2-SV(P) level with the SMD (*t*-BuOH) method. These TSs with various conformations were re-optimized at the ωB97X-D/Def2SVP level with the SMD (*t*-BuOH) method. All these DFT calculations were carried out with Gaussian 09 program.
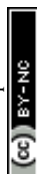
Conclusions

Triggered by the incidental finding of zinc(II)-promoted activation of alkynes, we explored intramolecular hydroarylations of *N*-propargylated tetrahydrocarbolines to develop a versatile synthetic process for generating scaffold and functional group variations. Protic and sterically demanding alcoholic solvents

such as *t*-BuOH dramatically accelerated the $Zn(OTf)_2$-promoted annulations. Computational investigations employing the AFIR method in the GRRM strategy provided a convincing rationale: *participation of t-BuOH as a proton donor plays a pivotal role in facilitating the protodezincation process.* The unique combination of $Zn(OTf)_2$ and *t*-BuOH allows the protodemetallation of alkenyl zinc species under mild and almost neutral conditions without the addition of Brønsted acid promoters.

We demonstrated that the modes of the $Zn(OTf)_2$-mediated cyclizations are controlled by appropriate choices of the reaction solvents and the substituents (R^1 and R^2) on the substrates **1a–f**. Divergent annulations involving two kinds of ring-expansion reactions and two dearomatizing spirocyclizations were systematically employed to gain programmable access to four distinct scaffolds: azepino[4,5-*b*]indole **2**, spirocycle **3**, azocino[5,4-*b*]indole **4**, and spirocyclic **5**. $Zn(OTf)_2$-mediated annulations of substrates **1a–c** bearing a terminal alkyne group allow divergent cyclizations between an internal alkyne carbon with either the indole C2 or C3 position to effect 7-*exo* cyclizations or 6-*exo* spirocyclizations, respectively. Notably, this study revealed that 6-*exo* dearomatizing spirocyclizations of **1c** resulting in formation of a quaternary center is a kinetically-favored pathway. Furthermore, treatment of the spirocyclic products **3a–c** with $Zn(OTf)_2$ under thermodynamic conditions can cause cascade reactions *via* migration of the alkenyl group and concomitant retro-Mannich-type fragmentation. Subsequent hydrolysis of the resulting iminium cation leads to irreversible formation of the azepino[4,5-*b*]indole scaffold **2a**. The R^1 substituents (Me, CO_2Me, CONHBn) of substrates **1a–c** were shown to greatly influence the susceptibilities of substrates for the irreversible reaction leading to **2a** at elevated temperature. In this cascade process, $Zn(OTf)_2$ could play key roles not only in the hydroarylation reaction (by activating the alkyne as a "π-acid") but also on alkenyl migration as a Lewis acid promoter for the imine group. In contrast to substrates **1a–c** which have a terminal alkyne and were converted to **2a** and **3a**, $Zn(OTf)_2$-mediated annulations of substrates **1d–f**, which have an internal alkyne, preferentially proceeded through the 8-*endo* ring expansion reaction to afford azocino[5,4-*b*]indole **4a** in good yield. Furthermore, substrate **1f** was demonstrated to affect the intriguing α-alkenylation of the carbonyl group to forge the tetracyclic scaffold **18** containing a quaternary carbon center and a trisubstituted olefin.

These experimental findings underscore that $Zn(OTf)_2$-mediated activation of alkynes provides relatively unexplored but versatile synthetic methodologies for the direct and flexible synthesis of skeletally diverse and densely-functionalized alkaloidal scaffolds reminiscent of natural products. The artificial force induced reaction method allows comprehensive discussion of transition states and could offer both rational and unanticipated guidelines for designing divergent reactions. Integration of synthetic strategies for generating skeletal variations with a systematic computational approach for identifying unforeseen reaction pathways could provide a new route for advancing the combinatorial chemical synthesis of functional molecules.

Conflicts of interest

There are no conflicts to declare.

Acknowledgements

Notes and references

1 (a) Y. Nakao, *Chem. Rec.*, 2011, **11**, 242–251; (b) A. Fürstner, *Acc. Chem. Res.*, 2014, **47**, 925–938; (c) Y. Yamamoto, *Chem. Soc. Rev.*, 2014, **43**, 1575–1600; (d) R. Dorel and A. M. Echavarren, *Chem. Rev.*, 2015, **115**, 9028–9072; (e) P. Gandeepan and C. H. Cheng, *Acc. Chem. Res.*, 2015, **48**, 1194–1206; (f) M. D. Greenhalgh, A. S. Jones and S. P. Thomas, *ChemCatChem*, 2015, **7**, 190–222; (g) R. Manikandan and M. Jeganmohan, *Org. Biomol. Chem.*, 2015, **13**, 10420–10436; (h) E. A. Standley, S. Z. Tasker, K. L. Jensen and T. F. Jamison, *Acc. Chem. Res.*, 2015, **48**, 1503–1514.

2 (a) X.-F. Wu and H. Neumann, *Adv. Synth. Catal.*, 2012, **354**, 3141–3160; (b) S. Enthaler, *ACS Catal.*, 2013, **3**, 150–158; (c) M. J. González, L. A. Lopez and R. Vicente, *Tetrahedron Lett.*, 2015, **56**, 1600–1608.

3 (a) S. Maeda, Y. Harabuchi, M. Takagi, T. Taketsugu and K. Morokuma, *Chem. Rec.*, 2016, **16**, 2232–2248; (b) W. M. Sameera, S. Maeda and K. Morokuma, *Acc. Chem. Res.*, 2016, **49**, 763–773.

4 (a) H. Mizoguchi, H. Oikawa and H. Oguri, *Nat. Chem.*, 2014, **6**, 57–64; (b) H. Mizoguchi, R. Watanabe, S. Minami, H. Oikawa and H. Oguri, *Org. Biomol. Chem.*, 2015, **13**, 5955–5963; (c) R. Watanabe, H. Mizoguchi, H. Oikawa, H. Ohashi, K. Watashi and H. Oguri, *Bioorg. Med. Chem.*, 2017, **25**, 2851–2855.

5 (a) C. Ferrer and A. M. Echavarren, *Angew. Chem., Int. Ed.*, 2006, **45**, 1105–1109; (b) C. Ferrer, C. H. M. Amijs and A. M. Echavarren, *Chem.–Eur. J.*, 2007, **13**, 1358–1373.

6 (a) S. G. Modha, D. D. Vachhani, J. Jacobs, L. Van Meervelt and E. V. Van der Eycken, *Chem. Commun.*, 2012, **48**, 6550–6552; (b) V. A. Peshkov, O. P. Pereshivko and E. V. Van der Eycken, *Adv. Synth. Catal.*, 2012, **354**, 2841–2848.

7 (a) L. Zhang, L. Chang, H. Hu, H. Wang, Z. J. Yao and S. Wang, *Chem.–Eur. J.*, 2014, **20**, 2925–2932; (b) L. Zhang, Y. Wang, Z. J. Yao, S. Wang and Z. X. Yu, *J. Am. Chem. Soc.*, 2015, **137**, 13290–13300.

8 (a) Y. Liu, W. Xu and X. Wang, *Org. Lett.*, 2010, **12**, 1448–1451; (b) G. Li and Y. Liu, *J. Org. Chem.*, 2010, **75**, 3526–3528; (c) A. S. K. Hashmi, W. Yang and F. Rominger, *Adv. Synth. Catal.*, 2012, **354**, 1273–1279; (d) J. D. Podoll, Y. Liu, L. Chang, S. Walls, W. Wang and X. Wang, *Proc. Natl. Acad. Sci. U. S. A.*, 2013, **110**, 15573–15578; (e) P. Michael Barbour, J. D. Podoll, L. J. Marholz and X. Wang, *Bioorg. Med. Chem. Lett.*, 2014, **24**, 5602–5605; (f) W. Xu, W. Wang and X. Wang, *Angew. Chem., Int. Ed.*, 2015, **54**, 9546–9549; (g) Y. Li, S. Zhu, J. Li and A. Li, *J. Am. Chem. Soc.*, 2016, **138**, 3982–3985; (h) D. Nishiyama, A. Ohara, H. Chiba, H. Kumagai, S. Oishi, N. Fujii and H. Ohno, *Org. Lett.*, 2016, **18**, 1670–1673; (i) P. M. Barbour, W. Wang, L. Chang, K. L. Pickard, R. Rais, B. S. Slusher and X. Wang, *Adv. Synth. Catal.*, 2016, **358**, 1482–1490; (j) Y. Zhu, W. He, W. Wang, C. E. Pitsch, X. Wang and X. Wang, *Angew. Chem., Int. Ed.*, 2017, **56**, 12206–12209; (k) Y. Zhu, L. Cleaver, W. Wang, J. D. Podoll, S. Walls, A. Jolly and X. Wang, *Eur. J. Med. Chem.*, 2017, **125**, 130–142; (l) N. Glinsky-Olivier, P. Retailleau and X. Guinchard, *Eur. J. Org. Chem.*, 2018, 5823–5829; (m) X. Zhang, B. N. Nakde, R. Guo, S. Yadav, Y. Gu and A. Li, *Angew. Chem., Int. Ed.*, 2019, **58**, 6053–6058.

9 (a) M. Nakamura, C. Liang and E. Nakamura, *Org. Lett.*, 2004, **6**, 2015–2017; (b) S. Morikawa, S. Yamazaki, Y. Furusaki, N. Amano, K. Zenke and K. Kakiuchi, *J. Org. Chem.*, 2006, **71**, 3540–3544; (c) C.-L. Deng, R.-J. Song, Y.-L. Liu and J.-H. Li, *Adv. Synth. Catal.*, 2009, **351**, 3096–3100; (d) X.-L. Fang, R.-Y. Tang, X.-G. Zhang, P. Zhong, C.-L. Deng and J.-H. Li, *J. Organomet. Chem.*, 2010, **696**, 352–356; (e) V. Srinivas, K. V. Sajna and K. C. Kumara Swamy, *Tetrahedron Lett.*, 2011, **52**, 5323–5326; (f) W. Hess and J. W. Burton, *Adv. Synth. Catal.*, 2011, **353**, 2966–2970; (g) G. Li and H. Nakamura, *Angew. Chem., Int. Ed.*, 2016, **55**, 6758–6761.

10 (a) P. A. Donets, K. Van Hecke, L. Van Meervelt and E. V. Van der Eycken, *Org. Lett.*, 2009, **11**, 3618–3621; (b) H. Mizoguchi, H. Oikawa and H. Oguri, *Org. Biomol. Chem.*, 2012, **10**, 4236–4242.

11 (a) S. Maeda and K. Morokuma, *J. Chem. Phys.*, 2010, **132**, 241102/1–241102/4; (b) S. Maeda and K. Morokuma, *J. Chem. Theory Comput.*, 2011, **7**, 2335–2345; (c) S. Maeda, K. Ohno and K. Morokuma, *Phys. Chem. Chem. Phys.*, 2013, **15**, 3683–3701; (d) S. Maeda, T. Taketsugu and K. Morokuma, *J. Comput. Chem.*, 2014, **35**, 166–173.

12 (a) R. Uematsu, S. Maeda and T. Taketsugu, *Chem.–Asian J.*, 2014, **9**, 305–312; (b) R. Uematsu, E. Yamamoto, S. Maeda, H. Ito and T. Taketsugu, *J. Am. Chem. Soc.*, 2015, **137**, 4090–4099; (c) K. K. Vong, S. Maeda and K. Tanaka, *Chem.–Eur. J.*, 2016, **22**, 18865–18872; (d) E. Yamamoto, S. Maeda, T. Taketsugu and H. Ito, *Synlett*, 2017, **28**, 1258–1267; (e) T. Yoshimura, S. Mori, S. Maeda, T. Taketsugu,
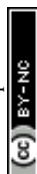
M. Sawamura and K. Morokuma, *Chem. Sci.*, 2017, **8**, 4475–4488.

13 The corresponding cyclization pathways to form the minor diastereomers such as *syn*-product **3a'** were also calculated to provide both a schematic and an energy profile for the reaction paths from **1a'** to **2a**/**3a'** (see ESI, Fig. S3 and S4†), although the minor *syn*-product **3a'** was not obtained experimentally.

14 S. Maeda, Y. Harabuchi, Y. Ono, T. Taketsugu and K. Morokuma, *Int. J. Quantum Chem.*, 2015, **115**, 258–269.

15 The crystallographic data (**3c**: CCDC-1905916, **4d**: CCDC-1905889, and **18**: CCDC-1905890).

16 (*a*) F. Dénès, A. Pérez-Luna and F. Chemla, *Chem. Rev.*, 2010, **110**, 2366–2447; (*b*) Y. Liu, R.-J. Song and J.-H. Li, *Synthesis*, 2010, 3663–3669; (*c*) W. Hessa and J. W. Burton, *Adv. Synth. Catal.*, 2011, **353**, 2966–2970; (*d*) D. Hack, M. Blümel, P. Chauhan, A. Philipps and D. Enders, *Chem. Soc. Rev.*, 2015, **44**, 6059–6093; (*e*) M. Cao, A. Yesilcimen and M. Wasa, *J. Am. Chem. Soc.*, 2019, **141**, 4199–4203.

17 J. P. Perdew, K. Burke and M. Ernzerhof, *Phys. Rev. Lett.*, 1996, **77**, 3865–3868.

18 F. Weigend and R. Ahlrichs, *Phys. Chem. Chem. Phys.*, 2005, **7**, 3297–3305.

19 *TURBOMOLE V7.0.1 2015*, A Development of University of Karlsruhe and Forschungszentrum Karlsruhe GmbH, 1989-2007, TURBOMOLE GmbH, Since 2007.

20 C. Choi and R. Elber, *J. Chem. Phys.*, 1991, **94**, 751–760.

21 A. D. Becke, *J. Chem. Phys.*, 1993, **98**, 5648–5652.

22 A. V. Marenich, C. J. Cramer and D. G. Truhlar, *J. Phys. Chem. B*, 2009, **113**, 6378–6396.

23 M. J. Frisch, G. W. Trucks, H. B. Schlegel, G. E. Scuseria, M. A. Robb, J. R. Cheeseman, G. Scalmani, V. Barone, B. Mennucci, G. A. Petersson, H. Nakatsuji, M. Caricato, X. Li, H. P. Hratchian, A. F. Izmaylov, J. Bloino, G. Zheng, J. L. Sonnenberg, M. Hada, M. Ehara, K. Toyota, R. Fukuda, J. Hasegawa, M. Ishida, T. Nakajima, Y. Honda, O. Kitao, H. Nakai, T. Vreven, J. A. Montgomery Jr, J. E. Peralta, F. Ogliaro, M. Bearpark, J. J. Heyd, E. Brothers, K. N. Kudin, V. N. Staroverov, T. Keith, R. Kobayashi, J. Normand, K. Raghavachari, A. Rendell, J. C. Burant, S. S. Iyengar, J. Tomasi, M. Cossi, N. Rega, J. M. Millam, M. Klene, J. E. Knox, J. B. Cross, V. Bakken, C. Adamo, J. Jaramillo, R. Gomperts, R. E. Stratmann, O. Yazyev, A. J. Austin, R. Cammi, C. Pomelli, J. W. Ochterski, R. L. Martin, K. Morokuma, V. G. Zakrzewski, G. A. Voth, P. Salvador, J. J. Dannenberg, S. Dapprich, A. D. Daniels, O. Farkas, J. B. Foresman, J. V. Ortiz, J. Cioslowski and D. J. Fox, *Gaussian 09, Revision D.01*, Gaussian, Inc., Wallingford CT, 2013.

24 J.-D. Chai and M. Head-Gordon, *Phys. Chem. Chem. Phys.*, 2008, **10**, 6615–6620.